Nutrient stoichiometry shapes microbial coevolution

Megan L. Larsen[1], Steven W. Wilhelm[2], Jay T. Lennon[*1]

Affiliations

[1]Department of Biology, Indiana University, Bloomington, IN 47405

[2]Department of Microbiology, University of Tennessee, Knoxville, TN 37996

*Correspondence to: lennonj@indiana.edu.

ABSTRACT

Coevolution arises from the reciprocal genetic change between species and represents a major evolutionary force that contributes to the generation and maintenance of biodiversity. The tempo and mode of coevolution are affected by environmental conditions that modify species interactions. For example, the scarcity of essential elements influences the nutrition and productivity of host populations, which should not only regulate parasite dynamics, but also drive the evolution of defense and virulence traits. To explore the effects of nutrient availability on antagonistic coevolution, we conducted a long-term chemostat experiment where the marine cyanobacterium *Synechococcus* was challenged with a lytic phage under nitrogen (N) or phosphorus (P) limitation. Our manipulation of nutrient stoichiometry influenced the stability of host-parasite interactions, but also affected the underlying mode of coevolution. By assessing infectivity with more than 18,000 pairwise challenges using time-shift and network analyses, we documented directional selection for increased phage resistance, a pattern that is consistent with coevolutionary arms-race dynamics. In contrast, phage infectivity fluctuated through time, as expected when coevolution is determined by negative frequency-dependent selection, but was 70 % higher on naive hosts that evolved under N-limitation versus P-limitation. Furthermore, infection networks were 25 % more modular under P-limitation than N-limitation reflecting host-range contraction and an asymmetric coevolutionary trajectory. Together, our results demonstrate that nutrient stoichiometry creates eco-evolutionary feedbacks that may alter the dynamics and functioning of environmental and host-associated microbial communities.

SIGNIFICANCE STATEMENT

34 As obligate parasites, phage represent a significant source of mortality for marine cyanobacteria, which are photosynthetic microorganisms that play a central role in the regulation
36 of biogeochemical processes, including energy flow, carbon sequestration, and the cycling of nitrogen (N) and phosphorus (P). Phage also act as agents of evolutionary change by selecting
38 for resistant cyanobacteria, which can give rise to counter-resistant phage. This coevolutionary process was differentially affected by the availability of N and P in ways that could impact the
40 ecology and evolution of one of the most abundant and functionally important groups of microorganisms on Earth.

42

\body

In order to grow and reproduce, organisms must assimilate elements from the environment to meet their nutritional and energetic demands. Ecological stoichiometry is a theoretical framework that explicitly considers the mass balance of materials and energy in the environment and the individuals that incorporate them (1). Of the approximately 25 elements contained in biomass, nitrogen (N) and phosphorus (P) are two of the most limiting and essential nutrients. N and P are needed for the synthesis of major macromolecules, including nucleic acids, ribosomes, proteins, and cellular membranes that collectively influence an organism's performance. However, the degree to which N and P are regulated greatly varies among major groups of taxa. For example, the biomass stoichiometry of primary producers tends to be flexible, reflecting the supply of nutrients in their environment (1). In contrast, the biomass stoichiometry of consumer populations is homeostatically regulated and therefore tends to remain constant even when the nutrient content of their resources fluctuates (1). Such differences can create a nutritional imbalance between primary producers and consumers, which has profound consequences for a wide range of ecological processes including resource competition, host-parasite dynamics, and ecosystem functioning (2-4).

Nutrient stoichiometry can also influence evolutionary processes. Nutrient limitation often leads to a reduction in population size, which can diminish the efficiency of selection and result in the accumulation of deleterious mutations through genetic drift (5). However, many populations have adaptations that allow individuals to contend with absolute and relative resource scarcity. For example, the disproportionate use of nucleotides that vary in N content reduces stoichiometric mismatch between an organism and its environment (6). Similarly, natural selection can operate on the material costs of gene expression in ways that lead to the

68 sparing of elements that are normally used in highly expressed proteins (7). These genetic responses to nutrient limitation may give rise to the evolution of organismal stoichiometry. For
70 example, long-term carbon limitation led to increases in the N and P content of experimentally evolved bacterial populations (8). However, evolutionary responses to nutrient stoichiometry
72 may depend on the identity of the limiting nutrient (9). While N limitation can select for stress-related or catabolic genes with lower guanine-cytosine content (10), P limitation can favor the
74 replacement of phospholipids with sulfolipids in the cell membranes of certain microorganisms (11).

76 In a community context, the combined effects of nutrient stoichiometry may give rise to eco-evolutionary feedbacks. Such feedbacks occur when ecological interactions affect
78 evolutionary processes, which in turn modify species interactions and ecological dynamics (12). For example, the rapid evolution of functional traits can produce diminished oscillations, longer
80 periods of cycling, and phase-shifted populations densities between hosts and their parasites, a phenomenon referred to as "cryptic dynamics" (13). Theory suggests that cryptic dynamics can
82 arise when nutrient stoichiometry alters the stability of antagonistic species interactions (14), which may ultimately intensify arms-race dynamics and negative frequency-dependent selection
84 (4). However, links among nutrient stoichiometry, eco-evolutionary feedbacks, and coevolution remain to be tested.

86 Major advances in evolutionary ecology have been made through experimental studies of microbial communities. In particular, bacteria and phage are ideal for studying eco-evolutionary
88 feedbacks owing to their large population sizes, rapid growth rates, and experimental tractability. Moreover, bacteria and phage dynamics are critical for understanding the structure and function
90 of microbial food webs, especially in aquatic ecosystems (15). For example, *Synechococcus* is a

diverse and widely distributed group of primary producers in the world ocean with an estimated
92 global abundance of 10^{26} cells (16). While *Synechococcus* must contend with both N- and P-
limitation, it is also subject to a high degree of phage-induced mortality, which can lead to
94 coevolutionary dynamics (17). These coevolutionary processes can create feedbacks that not
only influence population dynamics, but also ecosystem functioning, including the turnover of N
96 and P (18).

In this study, we tested how nutrient stoichiometry affects host-parasite eco-evolutionary
98 dynamics in an experiment where a single genotype of marine *Synechococcus* was infected with
a phage strain in chemostats that were supplied with either N- or P-limited media. We isolated
100 hundreds of host and phage strains, which were challenged against one another to document
phenotypic changes in resistance and infectivity over the course of the experiment. Based on the
102 results from time-shift and network analyses, our data reveal that nutrient stoichiometry is a
bottom-up force that regulates eco-evolutionary feedbacks in ways that alter coevolutionary
104 processes.

106

RESULTS AND DISCUSSION

108 Our results demonstrate that the relative amounts of nitrogen (N) and phosphorus (P) in
an environment have strong eco-evolutionary effects on marine *Synechococcus* and its phage.
110 Communities were more stable under P-limitation than N-limitation, which likely was influenced
by the stoichiometric constraints and elemental homeostasis of the host and phage populations.
112 In addition to the importance of these ecological processes, resistant cyanobacteria rapidly
invaded the community, which was followed by the appearance of evolved phage with altered
114 host-ranges. The resulting patterns of resistance and infectivity were different among N- and P-

limited treatments suggesting that nutrient stoichiometry altered coevolutionary dynamics. Using
116 time-shift assays and network analyses, we detected strong signatures of arms-race dynamics in both nutrient treatments. However, under P-limitation, we also observed patterns consistent with
118 negative frequency-dependent selection, which may reflect the underlying costs of maintaining defense and virulence traits in different nutrient environments. Our findings generate testable
120 predictions regarding the coevolutionary mechanisms of local adaptation for microorganisms found among oceans where N : P stoichiometry in known to systematically vary (19).
122

Eco-evolutionary effects of stoichiometry on community dynamics — Consistent with
124 predictions from the theory of ecological stoichiometry (1), we documented that *Synechococcus* and phage dynamics were highly sensitive to variation in nutrient supply (RM-ANOVA; time x
126 stoichiometry, $P < 0.0001$). Under N-limitation, *Synechococcus* rapidly declined reaching its minimum density 35 ± 11.2 days following phage addition ($1.7 \times 10^5 \pm 6.54 \times 10^4$ cells mL^{-1},
128 mean ± SEM, Fig. 1a, Table S4). This reduction in host abundance corresponded with a spike in phage density, which peaked near 25 ± 8.0 days ($8.5 \times 10^8 \pm 1.40 \times 10^8$ particles mL^{-1}, mean ±
130 SEM). Over the next 50 days, host densities slowly recovered, and entered a second round of decline near day 100. In contrast, communities were more stable under P-limitation
132 (*Synechococcus*: *t*-test, $t_4 = -3.38$, $P = 0.04$; *t*-test, phage: $t_4 = 3.15$, $P < 0.001$, Fig. 1b, Table S4). Hosts declined more slowly following phage addition (*t*-test, $t_4 = -4.00$, $P = 0.02$) and reached
134 their minimum density ($4.0 \times 10^5 \pm 5.74 \times 10^4$ cells mL^{-1}, mean ± SEM) near 78 ± 15.6 days. Meanwhile, phage populations remained high and relatively constant ($2.4 \times 10^8 \pm 9.45 \times$
136 10^7 particles mL^{-1}, mean ± SEM) throughout the duration of the experiment. Nutrient stoichiometry also affected the synchrony of the microbial populations within a chemostat.
138 While host and phage densities were out-of-phase with a lag of two to four days in N-limited

chemostats (r = -0.22 to -0.14, $P < 0.001$, Figs. 1, S1), there was no detectable coherence
140 between *Synechococcus* and phage experiencing P-limitation over the course of the experiment (r = -0.04 to 0.013, $P > 0.50$, Figs. 1, S1).

142 Historically, ecologists have attempted to explain variation in population and community dynamics assuming a single currency of resource. However, systems can exhibit a much wider
144 range of behaviors when resource stoichiometry is explicitly considered owing to feedbacks that arise when interacting species vary in the degree to which their elemental composition is
146 homeoestatically regulated (20). For example, the molar N : P ratio of marine *Synechococcus* converges upon the canonical Redfield value of 16 : 1 in some environments (21), but in other
148 instances can exceed 100 : 1 (22)reflecting the extremely plasticity of its biomass stoichiometry. In contrast, phage are thought to have a fixed elemental composition owing to their relatively
150 simple structure, which minimally consists of genetic material (DNA or RNA) protected by a proteinaceous capsid (23). Unless they contain auxiliary metabolic genes that allow for
152 redirection of resources (24), phage are entirely dependent on the stoichiometry of their host when assembling new viruses. Biophysical models predict that the T4-like phage used in our
154 study have a high P demand due to their low N : P ratio of approximately 7 : 1 (23). As a consequence, phage productivity is thought to be constrained by host P content. For example,
156 host lysis was delayed by 18 hrs leading to an 80 % reduction in phage burst size when P-limited *Synechococcus* WH7803 was infected with a myorvirus (25). Such findings suggest that nutrient
158 stoichiometry can profoundly shape host-phage dynamics and provide an ecological explanation for the contrasting dynamics observed in our study (Fig. 1).

160 In addition, nutrient stoichiometry may affect community dynamics by generating eco-evolutionary feedbacks. Such feedbacks arise when there are rapid changes in host or parasite

162 traits leading to cryptic dynamics, which are not predicted from traditional ecological theory (13). Cryptic dynamics require the coexistence of multiple host genotypes that exhibit trade-offs
164 in competitive ability and parasite defense (13). While there are many intracellular and extracellular mechanisms that bacteria can employ to resist phage infection, *Synechococcus*
166 appears to undergo mutations of receptors on the cell surface that reduce or eliminate attachment, thus precluding entry of the virus into the host (26). Resistance mutations in *Synechococcus* are
168 often accompanied by a reduction in growth rate, the magnitude of which can vary depending on the identity of the host and virus (27). These fitness costs have important consequences for
170 understanding community stability. Without a reduction in growth rate, resistant *Synechococcus* would outcompete the sensitive host and drive the phage population extinct. Moreover, fitness
172 costs establish a trade-off that satisfies the requirement for cryptic dynamics to emerge (13). In sum, our data support the view that nutrient stoichiometry altered host-phage dynamics and
174 stability via eco-evolutionary feedbacks.

176 **Nutrient-dependent coevolution —** Nutrient stoichiometry had strong, but asymmetric effects on microbial coevolution. Phage-resistant cyanobacteria rapidly arose and swept through the
178 population over the course of the experiment (Fig. S2). Within nine days of phage addition, ~30 % of the *Synechococcus* strains were resistant to the ancestral phage in both the N- and P-limited
180 chemostats. Although average resistance continued to increase over time (RM-ANOVA, $F_{6, 97}$ = 14.27, $P < 0.001$), it was not affected by nutrient stoichiometry ($F_{6, 97} = 0.51$, $P = 0.30$). In
182 contrast, changes in phage infectivity were significantly altered by nutrient stoichiometry. For example, we recovered a host-range mutant from a P-limited chemostat (day 129) that was able
184 to infect a *Synechococcus* strain (day 166), which was resistant to the ancestral phage. In

addition, three phage strains from N-limited chemostats and two phage strains from P-limited
186 chemostats (day 166) were able to infect phage-resistant *Synechococcus* isolated from other chemostats earlier in the study. Overall, phage from the N-limited chemostats were 12 % more
188 infective than phage from the P-limited chemostats (RM-ANOVA, stoichiometry x time: $F_{4, 166} = 4.83$, $P = 0.001$). These effects of nutrient stoichiometry on host-phage interactions led us to
190 further explore the potential mechanism and patterns underlying the observed coevolution in our system.

192 There are two primary modes by which antagonistic coevolution is thought to occur. The first is through arms-race dynamics involving gene-for-gene specificity, where directional
194 selection leads to an escalation of resistance and infectivity. Arms-race dynamics were originally described for coevolving populations of plants and pathogens, but since then have been
196 commonly reported in studies of bacteria and phage (28, 29). The second mode of antagonistic co-evolution involves negative frequency-dependent selection where parasites evolve to infect
198 common hosts, which in turn favors rare host alleles. Negative frequency-dependent selection is often associated with infections that require matching alleles and is well documented in
200 invertebrate systems (30), but has also been described in some studies of bacteria and phage(31). While arms-race dynamics and negative frequency-dependent selection are often viewed as
202 occupying different ends of the coevolutionary spectrum, they are not mutually exclusive (32). In fact, evidence suggests that over time, arms-race dynamics can give way to negative frequency-
204 dependent selection, in some cases depending on resource availability (33).

One powerful way to discern modes of coevolution is through the use of time-shift
206 analyses. This approach involves determining the success of infections for combinations of hosts and parasites that are isolated from different time points in a controlled experiment or other

208 longitudinal type of study (34). When applied to our chemostat data, time-shift analyses indicated that coevolutionary dynamics were significantly affected by nutrient stoichiometry

210 (Fig. 3, RM-ANOVA, stoichiometry x time, $F_{1, 601} = 4.26$, $P = 0.039$). Specifically, when hosts isolated from the phage-amended chemostats were challenged against current and past phage,

212 infectivity was weak owing to the evolution of phage resistance (Fig. 3 a, b). Infectivity was stronger when hosts were challenged against future phage, but only for *Synechococcus* strains

214 that were isolated earlier in the experiment (days -6, 9, and 23). Consistent with arms-race dynamics, these patterns reflect escalating resistance in the host population that were not affected

216 nutrient stoichiometry (Fig. 3 a, b; stoichiometry x time shift, $F_{1, 602} = 0.05$, $P = 0.82$). We obtained additional insight by conducting time-shift analyses with *Synechococcus* that were

218 isolated from no-phage control chemostats (Fig. 3 c, d; stoichiometry x time shift, $F_{1, 289} = 10.3$, $P = 0.0015$). In contrast to initial expectations, phage infectivity was not uniformly high on these

220 naive hosts, but rather fluctuated over time (Fig. 3 c, d) owing in part to host-range contraction. We also found that infectivity was 70 % stronger under N-limitation (0.61 ± 0.289) than P-

222 limitation (0.36 ± 0.332), which together is consistent with nutrient-dependent coevolution that was driven by negative frequency-dependent selection.

224 Network analyses provide an additional way to evaluate the effects of nutrient stoichiometry on the mode of coevolution. With this approach, one can estimate the degree of

226 nestedness that exists among pairs of hosts and phage relative to randomized data. Often, infection data from bacteria-phage systems are highly nested (35), which means they contain

228 ordered subsets of phenotypes whereby hosts from later time points are resistant to earlier phages, and phage from later time points are able to infect earlier hosts (36). In our study,

230 infection networks were significantly nested, a pattern that arises from arms-race dynamics.

However, the degree of nestedness was not affected by nutrient stoichiometry (NODF, $t_4 = 0.37$,
232 $P = 0.72$, Table S5). Infection networks can also exhibit modularity, which is more consistent
with negative frequency-dependent selection(36). Modules reflect dense clusters of interacting
234 host and phage compared to other strain combinations found in a bipartite infection matrix.
Although less commonly documented, modularity has been observed in large-scale oceanic
236 surveys of bacteria and phage, but has been attributed local adaptation and the phylogenetic
breadth of the hosts (37). However, theory suggests that modularity can emerge *via* coevolution
238 between two populations at the local scale. Using a "relaxed lock and key" model,
simultaneously nested and modular structures arose under simple chemostat conditions that
240 assumed gene matching between phage tail-fibers and host receptors (38). Our results are in
agreement with these predictions, but suggest that network properties are affected by host
242 nutrition. Specifically, we found that host-phage interactions were 50 % more modular under P-
limitation than N-limitation ($t_{3.0018} = -3.55$, $P = 0.038$, Fig. 4, Table S5,) suggesting that nutrient
244 stoichiometry constrains host-phage interactions leading to increased specialization. Such
findings are consistent with the view that resources can influence the modes of coevolution based
246 in part on the fitness costs associated with host defense and infection strategies (33)

Mechanistically, there are many ways that nutrient stoichiometry could shape bacteria-
248 phage coevolution. For example, the "dangerous nutrients" hypothesis predicts that trajectories
of coevolution can be influenced when receptors used by nutrient-limited hosts also serve as the
250 targets of phage adsorption (39). However, it does not appear that myoviruses, including the
strain used in this study, attach to the protein receptors of cyanobacteria that are used for nutrient
252 transport. Instead, evidence from whole-genome sequencing suggests that phage-resistant
Synechococcus accumulate mutations in hypervariable genomic islands that encode for

254 lipopolysaccharide (LPS) (17), a major component of the outer membrane in Gram-negative bacteria. The structural complexity of LPS is affected by nutrient limitation (40) and such
256 changes in molecular structure of the cell membrane can interfere with phage adsorption leading to resistance (41). Nevertheless, modification of tail-fibers allow phage to overcome resistance of
258 marine cyanobacteria in some instances (42) while the acquisition of host-like P-assimilation genes may aid in the successful infection of nutrient-limited hosts (43).

260

Conclusions — Most organisms live in environments where they are limited by the relative or
262 absolute amount of one or more essential resources. It is well established that such variation in nutrient stoichiometry can regulate ecological phenomena ranging from species interactions to
264 ecosystem-level processes. We demonstrated that nutrient stoichiometry also affects the eco-evolutionary dynamics of microbial communities through directional selection for increased
266 phage resistance and the evolution of host-range mutations. Identifying the targets of selection in contrasting nutrient environments will help elucidate the genetic mechanisms of coevolution and
268 the trade-offs associated with defense and virulence traits. Such findings will provide valuable insight into the evolutionary ecology of marine food webs. While our study offers promising
270 avenues to better understand bacteria-phage interactions in the oceans, nutrient stoichiometry is also important in determining the nutrition, health, and disease susceptibility for for non-
272 microbial hosts (2). By considering the ecology and evolutionary effects of nutrient stoichiometry, we may be able to better manage the persistence, emergence, and evolution of
274 infectious diseases.

276 **MATERIALS AND METHODS**

Strains and media — We evaluated the effects of nutrient stoichiometry on the eco-
278 evolutionary dynamics of the marine cyanobacterium *Synechococcus* WH7803 and a lytic T4-
like phage belonging to the Myoviridae family of phage (SRIM8). Changes to nutrient supply
280 can alter the equilibrium density of microbial populations in continuous culture (chemostats),
which in turn, may affect cyanobacteria-phage contact rates (45). Therefore, we adjusted both the
282 concentrations and ratios of N and P in modified AN artificial seawater medium (Tables S1-S3)
to induce N- or P-limitation while maintaining similar equilibrium densities of *Synechococcus*
284 between the stoichiometry treatments prior to phage addition. Specifically, the N-limited
medium had an N : P ratio of 10 : 1 (KNO_3; N = 220 μM) while the P-limited medium had a N :
286 P ratio of 40 : 1 (K_2HPO_4; P = 11 μM). Growth assays confirmed that *Synechococcus* was
limited by N under low N : P supply and by P under high N : P supply (see Fig. S3).
288

Chemostat experiment — We supplied ten chemostats, each with a 40 mL operating volume,
290 with N-limited or P-limited medium at a dilution rate of 1 d^{-1} (Tables S1-S3). The chemostats
were maintained in a Percival growth chamber (Perry, IA, USA) at 25 °C on a 14:10 light : dark
292 cycle under 20 μE m^{-2} s^{-1} and homogenized with magnetic stir bars following inoculation with a
single-colony strain of *Synechococcus* WH7803. We allowed the *Synechococcus* populations to
294 equilibrate in the chemostats for 125 d prior to initiating the "phage-amended" treatment by
introducing an aliquot of a plaque-purified S-RIM8 to three randomly chosen chemostats in each
296 nutrient treatment to achieve a multiplicity of infection (phage : cyanobacteria ratio) of
approximately 10. To document the potential influence of stoichiometry on population dynamics
298 and population size, we maintained two "no phage" chemostats with only *Synechococcus* in both
stoichiometry treatments (Fig. S4).

300

Community dynamics — We tracked *Synechococcus* and phage densities in each chemostat via
302 epifluorescent microscopy every other day for 172 days. *Synechococcus* populations were enumerated by concentrating samples from a chemostat onto 0.22-μm nominal pore-size black
304 polycarbonate filters. After removing cellular material (0.2 μm filtration) and extracellular DNA with DNase I, we concentrated samples onto 0.02 μm Anodisc filters for phage enumeration.
306 Each phage-containing filter was then stained with SYBR Green I. We captured and analyzed ten images from each filter with a CY3 filter set (ex: 550 nm, em: 570 nm) for *Synechococcus* or a
308 FITC filter set (ex: 497 nm, em: 520 nm) for phage using a Zeiss microscope and Axiovision imaging software (Release 4.5 SP1).

310 We evaluated the effects of nutrient stoichiometry on *Synechococcus* and phage dynamics in three ways. First, we tested for the main and interactive effects of nutrient
312 stoichiometry using repeated measures (RM) ANOVA. Second, because cryptic dynamics can alter the degree of synchrony between hosts and parasites, we performed cross-correlation
314 analyses on pre-whitened population data using Auto Regressive Integrated Moving Average (ARIMA) procedures in SAS (18). Last, we estimated the effects of nutrient stoichiometry on the
316 stability of *Synechococcus* and phage populations as the inverse of the coefficient of variation (CV) over time using *t*-tests.

318

Co-evolutionary dynamics — To test for the effects of nutrient stoichiometry on phenotypic
320 coevolution, we tracked changes in infection patterns between *Synechococcus* and its phage over time. We isolated multiple (3-5) *Synechococcus* strains from each chemostat using dilution-to-
322 extinction techniques six days prior to phage addition (day -6) and at days 9, 23, 72, 129, 148,

and 166 after phage addition. Single-colony strains of *Synechococcus* were harvested near mid-
324 log phase then concentrated *via* centrifugation, preserved in glycerol (10 % final concentration), and stored at -80 °C until reanimation. We also isolated multiple (3-5) phage strains from the
326 phage-amended chemostats on days 23, 72, 129, 148, and 166 through plaque purification using ancestral *Synechococcus* WH7803 as the host. Each 1 µm syringe-filtered phage lysate was
328 preserved in glycerol (10 % final concentration) at -80 °C.

With the isolated chemostat strains, we quantified host resistance and phage infectivity
330 using challenge assays. Each pair-wise challenge was completed in triplicate by adding 20 µL of a phage stock (~10^7 particles mL^{-1}) to 200 µL of a dilute *Synechococcus* strain (~10^6 cells mL^{-1})
332 in 96-well plates. Challenge assays were performed using the same medium from which the host strain was originally isolated. Turbid cultures of *Synechococcus* WH7803 appear bright pink
334 owing to the intracellular photosynthetic pigment phycoerythrin. When infected by SRIM8, however, cells are lysed and cultures become clear (18). Based on this, we scored each
336 *Synechococcus* strain as resistant (and the phage strain as infective) if there was a lack of growth after a two-week incubation under continuous light (20 µE m^{-2} s^{-1}) at 25 °C compared to control
338 wells (n = 3) that contained heat-killed phage. In total, there were 18,050 pairwise challenges between chemostat-isolated strains of *Synechococcus* and phage that resulted in a bipartite
340 infection matrix, which we used for all analyses related to phenotypic coevolution.

To quantify the effect of stoichiometry on coevolutionary dynamics, first, we used RM-
342 ANOVA to test for trends in average resistance and average infectivity over the course of the chemostat experiment. Second, we used the infection matrix to perform time-shift analyses,
344 which involved calculating the proportion of successful infections that occurred between hosts that were challenged against past, contemporary, and future phage strains (34). We statistically

346 analyzed the time-shift data using RM-ANOVA with nutrient treatment, phage treatment, and time as fixed effects, while the chemostat replicate identifier was treated as a random effect with
348 a corARMA covariance matrix (46). To visualize the data, contemporary challenges were centered at a time-shift of zero, while interactions with past phage were represented in negative
350 space and future interactions were represented in positive space. Last, to gain insight into potential mechanisms underlying stoichiometrically driven coevolution, we used community
352 network analyses to calculate the connectance, nestedness, and modularity for each chemostat infection matrix. Connectance was calculated as the number of interactions divided by network
354 size. We calculated nestedness using the NODF metric, which ranges from 0 (non-nested) to 1 (perfectly nested) and normalizes for matrix size. We used the LP-BRIM algorithm to find the
356 partition that maximizes Barber's modularity (Qb), which ranges from 0 (all interactions are between modules) to 1 (all interactions are within modules). The network statistics were
358 calculated using 100,000 random Bernoulli simulations in the BiWeb package for MATLAB (35, 47, http://github.com/tpoisot/BiWeb). We then tested for differences in connectance, nestedness,
360 and modularity between the nutrient treatments using *t*-tests.

362 **Available code and data.** Data and code are available in the public GitHub repository https://github.com/LennonLab/eco-evo-stoich

364

Author contributions

366 MLL, SWW, and JTL designed study; MLL performed research; MLL and JTL analyzed data; MLL, SWW, and JTL wrote paper.

368

Acknowledgments

We acknowledge technical support from R Morrison, M Carroll, and BK Lehmkuhl; ancestral strains from MF Marston; discussion with CM Lively; feedback from BK Whitaker, KJ Locey, WR Shoemaker, NI Wisnoski, V Kuo, ME Muscarella, DA Schwartz, RZ Moger-Reischer, JM Palange on earlier versions of the manuscript. Financial support was provided by the National Science Foundation (0851143, 0851113) and the US Army Research Office Grant W911NF-14-1-0411. We dedicate this work to the memory of VH Smith.

REFERNCES

378 1. Sterner RW & Elser JJ (2002) *Ecological Stoichiometry: The Biology of Elements from Molecules to the Biosphere* (Princeton University Press).

380 2. Smith VH & Holt RD (1996) Resource competition and within-host disease dynamics. *Trends Ecol Evol* 11(9):386-389.

382 3. Hall SR (2009) Stoichiometrically Explicit Food Webs: Feedbacks between resource supply, elemental constraints, and species diversity. *Annu Rev Ecol Evol Syst* Vol 40, pp
384 503-528.

4. Aalto SL, Decaestecker E, & Pulkkinen K (2015) A three-way perspective of
386 stoichiometric changes on host-parasite interactions. *Trends Parasitol* 31(7):333-340.

5. Kimura M (1962) On the probability of fixation of mutant genes in a population.
388 *Genetics* 47:713-719.

6. Elser JJ, Acquisti C, & Kumar S (2011) Stoichiogenomics: the evolutionary ecology of
390 macromolecular elemental composition. *Trends Ecol Evol* 26(1):38-44.

7. Bragg JG & Wagner A (2009) Protein material costs: single atoms can make an
392 evolutionary difference. *Trends in Genet* 25(1):5-8.

8. Turner CB, Wade BD, Meyer JR, Sommerfeld BA, & Lenski RE (2017) Evolution of
394 organismal stoichiomery in a long-term experiment with *Escherichia coli*. *R. Soc. Open Sci.* DOI: 10.1098/rsos.170497

396 9. Gresham D*, et al.* (2008) The repertoire and dynamics of evolutionary adaptations to controlled nutrient-limited environments in yeast. *PLoS Genetics* 4(12).

398 10. Acquisti C, Elser JJ, & Kumar S (2009) Ecological mitrogen limitation shapes the DNA composition of plant genomes. *Mol Biol Evol* 26(5):953-956.

400 11. Van Mooy BAS, Rocap G, Fredricks HF, Evans CT, & Devol AH (2006) Sulfolipids dramatically decrease phosphorus demand by picocyanobacteria in oligotrophic marine
402 environments. *Proc Natl Acad Sci USA* 103(23):8607-8612.

12. Haloin JR & Strauss SY (2008) Interplay between ecological communities and evolution.
404 *Ann NY Acad Sci* 1133:87-125.

13. Yoshida T*, et al.* (2007) Cryptic population dynamics: Rapid evolution masks trophic
406 interactions. *PLoS Biol* 5(9):1868-1879.

14. Yamamichi M, Meunier CL, Peace A, Prater C, & Rua MA (2015) Rapid evolution of a
408 consumer stoichiometric trait destabilizes consumer-producer dynamics. *Oikos* 124(7):960-969.

410 15. Suttle CA (2007) Marine viruses - major players in the global ecosystem. *Nat Rev Microbiol* 5(10):801-812.

412 16. Flombaum P*, et al.* (2013) Present and future global distributions of the marine Cyanobacteria *Prochlorococcus* and *Synechococcus*. *Proc Natl Acad Sci USA*
414 110(24):9824-9829.

17. Marston MF*, et al.* (2012) Rapid diversification of coevolving marine *Synechococcus* and
416 a virus. *Proc Natl Acad Sci USA* 109(12):4544-4549.

18. Lennon JT & Martiny JBH (2008) Rapid evolution buffers ecosystem impacts of viruses
418 in a microbial food web. *Ecol Lett* 11(11):1178-1188.

19. Galbraith ED & Martiny AC (2015) A simple nutrient-dependence mechanism for
420 predicting the stoichiometry of marine ecosystems. *Proc Natl Acad Sci USA* 112(27):8199-8204.

422 20. Andersen T, Elser JJ, & Hessen DO (2004) Stoichiometry and population dynamics. *Ecol Lett* 7(9):884-900.

424 21. Garcia NS, Bonachela JA, & Martiny AC (2016) Interactions between growth-dependent changes in cell size, nutrient supply and cellular elemental stoichiometry of marine
426 *Synechococcus*. *ISMEJ* 10(11):2715-2724.

22. Bertilsson S, Berglund O, Karl DM, & Chisholm SW (2003) Elemental composition of
428 marine *Prochlorococcus* and *Synechococcus*: Implications for the ecological stoichiometry of the sea. *Limnol Oceanogr* 48(5):1721-1731.

430 23. Jover LF, Effler TC, Buchan A, Wilhelm SW, & Weitz JS (2014) The elemental composition of virus particles: implications for marine biogeochemical cycles. *Nat Rev*
432 *Microbiol* 12(7):519-528.

24. Monier A*, et al.* (2017) Host-derived viral transporter protein for nitrogen uptake in
434 infected marine phytoplankton. *Proc Natl Acad Sci USA* doi: 10.1073/pnas.1708097114

25. Wilson WH, Carr NG, & Mann NH (1996) The effect of phosphate status on the kinetics
436 of cyanophage infection in the oceanic cyanobacterium *Synechococcus* sp WH7803. *J Phycol* 32(4):506-516.

438 26. Stoddard LI, Martiny JBH, & Marston MF (2007) Selection and characterization of cyanophage resistance in marine *Synechococcus* strains. *Appl Environ Microbiol*
440 73(17):5516-5522.

27. Lennon JT (2007) Is there a cost of viral resistance in marine cyanobacteria? *ISMEJ*
442 1:300-312.

28. Dennehy JJ (2012) What can phages tell us about host-pathogen coevolution? *Int J Evol*
444 *Biol.* 2012:396165.

29. Koskella B & Brockhurst MA (2014) Bacteria-phage coevolution as a driver of
446 ecological and evolutionary processes in microbial communities. *FEMS Microbiol Rev* 38(5):916-931.

448 30. Decaestecker E*, et al.* (2007) Host-parasite 'Red Queen' dynamics archived in pond sediment. *Nature* 450(7171):870-U816.

450 31. Hall AR, Scanlan PD, Morgan AD, & Buckling A (2011) Host-parasite coevolutionary arms races give way to fluctuating selection. *Ecol Lett* 14(7):635-642.

452 32. Agrawal A & Lively CM (2002) Infection genetics: gene-for-gene versus matching-alleles models and all points in between. *Evol Ecol Res* 4(1):79-90.

454 33. Pascua LL*, et al.* (2014) Higher resources decrease fluctuating selection during host-parasite coevolution. *Ecol Lett* 17(11):1380-1388.

456 34. Gaba S & Ebert D (2009) Time-shift experiments as a tool to study antagonistic coevolution. *Trends Ecol Evol* 24(4):226-232.

458 35. Flores CO, Meyer JR, Valverde S, Farr L, & Weitz JS (2011) Statistical structure of host-phage interactions. *Proc Natl Acad Sci USA* 108(28):E288-E297.

460 36. Weitz JS*, et al.* (2013) Phage-bacteria infection networks. *Trends Microbiol* 21(2):82-91.

37. Flores CO, Valverde S, & Weitz JS (2013) Multi-scale structure and geographic drivers
462 of cross-infection within marine bacteria and phages. *ISMEJ* 7(3):520-532.

38. Beckett SJ & Williams HTP (2013) Coevolutionary diversification creates nested-
464 modular structure in phage-bacteria interaction networks. *Interface Focus* 3(6).

39. Menge DNL & Weitz JS (2009) Dangerous nutrients: Evolution of phytoplankton
466 resource uptake subject to virus attack. *J Theor Biol* 257(1):104-115.

40. Brelles-Mariño G & Boiardi JL (1997) Nitrogen limitation of chemostat-grown *Rhizobium etli* elicits higher infection-thread formation in *Phaseolus vulgaris* *Microbiology* 142(5):1067-1070.

41. León M & Bastías R (2015) Virulence reduction in bacteriophage resistant bacteria. *Front Microbiol* 6. doi:10.3389/fmicb.2015.00343

42. Schwartz DA & Lindell D (2017) Genetic hurdles limit the arms race between *Prochlorococcus* and the T7-like podoviruses infecting them. *ISMEJ* 11(8):1836-1851.

43. Kelly L, Ding HM, Huang KH, Osburne MS, & Chisholm SW (2013) Genetic diversity in cultured and wild marine cyanomyoviruses reveals phosphorus stress as a strong selective agent. *ISMEJ* 7(9):1827-1841.

44. Marston MF & Sallee JL (2003) Genetic diversity and temporal variation in the cyanophage community infecting marine *Synechococcus* species in Rhode Island's coastal waters. *Appl Environ Microbiol* 69(8):4639-4647.

45. Rhee GY (1978) Effects of N:P atomic ratios and nitration limitation on algal growth, cell composition, and nitrate uptake. *Limnol Oceanogr* 23(1):10-25.

46. Koskella B (2014) Bacteria-phage interactions across time and space: merging local adaptation and time-shift experiments to understand phage evolution. *Am Nat* 184:S9-S21.

47. Flores CO, Poisot T, Valverde S, & Weitz JS (2016) BiMat: a MATLAB package to facilitate the analysis of bipartite networks. *Methods Ecol Evol* 7(1):127-132.

490 **FIGURE CAPTIONS**

Fig. 1. Microbial community dynamics were affected by nutrient stoichiometry. *Synechococcus*
492 and phage densities were tracked in replicate (n = 3) chemostats receiving N- or P-limited media.
Vertical lines at day 0 indicate time of phage amendment. See Fig. S4 for *Synechococcus*
494 dynamics in the no-phage control chemostats. Data are represented as mean ± SEM.

496 **Fig. 2** Phenotypic co-evolution between hosts (*Synechococcus*) and phage was affected by
nutrient stoichiometry. We calculated infectivity based on the proportion of successful infections
498 between *Synechococcus* strains and phage strains that were isolated from chemostats at different
time points. Infectivity is proportional to the width of the edges (lines) connecting nodes
500 (symbols). Black squares correspond to phage isolated from the phage-amended chemostats,
white circles correspond to *Synechococcu*s isolated from phage-amended chemostats, and grey
502 circles correspond to naive *Synechococcus* isolated from no-phage control chemostats. The
absence of a line indicates that *Synechococcus* isolates were resistant to a particular phage
504 challenge.

506 **Fig. 3.** Time-shift analysis of host-phage infectivity reveals the effects of stoichiometry on
coevolution. Contemporary interactions (i.e., those between a host and phage strain isolated at
508 the same time point) are centered at time zero (grey vertical line) along the time-shift
(horizontal) axis. Interactions with past phage are shifted to the left (negative values) and
510 interactions with future phage are shifted to the right (positive values). Each black line
corresponds with the mean infectivity for *Synechococcus* isolated from a specific time point as
512 indicated by the open circle containing the isolation day (-6, 9, 23, 72, 100, 129, or 166). When

comparing challenges between hosts and phage from phage-amended chemostats (a, b),
514 infectivity was weak for hosts that were isolated after day 23 or when challenged against phage
from the past owing to the evolution of resistance. Such findings are consistent with arms-race
516 dynamics where directional selection gives rise to escalating host resistance. We also challenged
phage against naive hosts from the no-phage control chemostats (c, d). From this, we found that
518 infectivity was significantly higher under N-limitation than P-limitation, but overall, was lower
than what would be expected under arms-race dynamics. Instead, the fluctuations in infectivity
520 with respect to time-shift are consistent with negative frequency-dependent selection and reflect
asymmetry in the coevolution between *Synechococcus* and phage.

522

Fig. 4. Host-phage infection networks based on interactions between *Synechococcus* and phage
524 isolates that coevolved under N- and P-limitation. Networks were significantly nested, consistent
with expectations of host-phage systems coevolving under arms-race dynamics. However, the
526 degree of nestedness was not affect by stoichiometry. Left panel: Networks were also
significantly modular when compared to randomized networks, but the degree of modularity was
528 significantly greater in P-limited networks. Right panel: Infection networks with interactions
(colored cells) rearranged using the LPBrim algorithm in BiWeb to reflect the modular structure.
530 Each colored grouping within a panel corresponds to a calculated module within the interaction
network of N-limited (a – c) or P-limited (d – f) chemostats.

532

534 **Fig. 1**

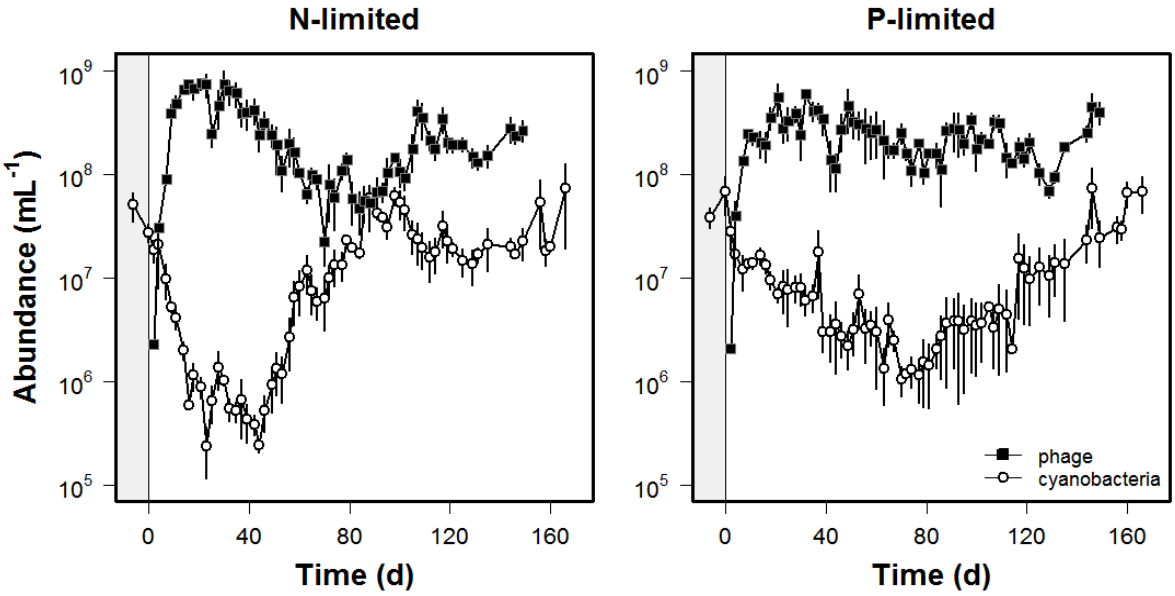

536

Fig. 1. Microbial community dynamics were affected by nutrient stoichiometry. Host (*Synechococcus*) and phage densities were tracked in replicate (n = 3) chemostats receiving N- or P-limited media. Vertical lines at day 0 indicate time of phage amendment. See Fig. S4 for *Synechococcus* dynamics in the no-phage control chemostats. Data are represented as mean ± SEM.

Fig. 2

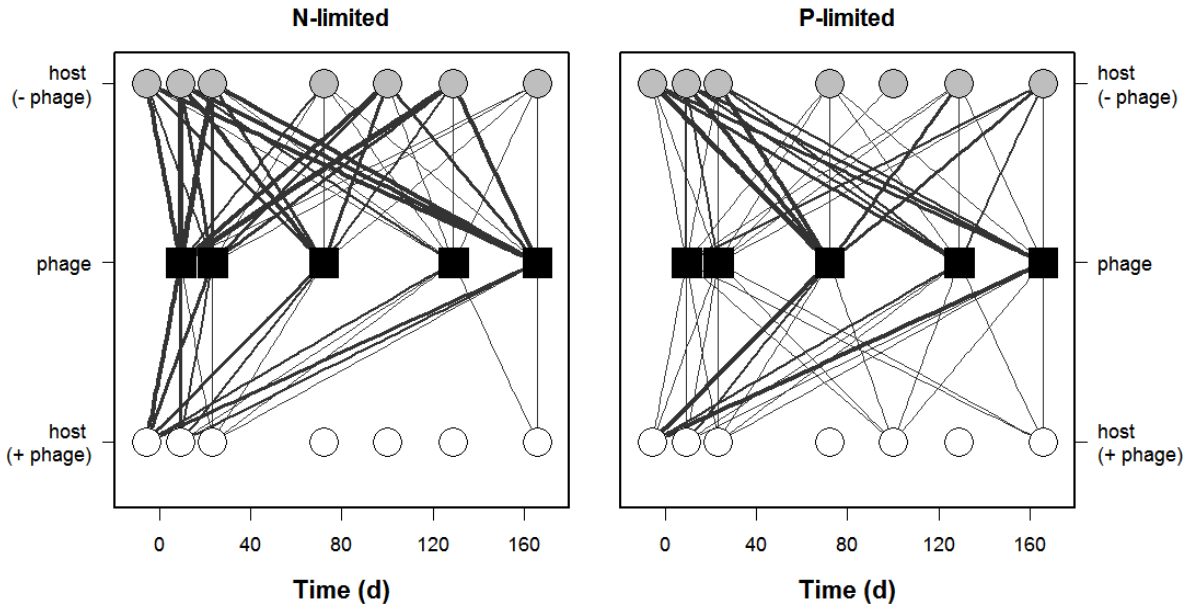

538

Figure 2 Phenotypic co-evolution based on infectivity of phage strains on *Synechococcus* strains isolated from N- and P-limited chemostats. We calculated infectivity based on the proportion of successful infections between hosts and phage that were isolated from chemostats at different time points. Infectivity is proportional to the width of the edges (lines) connecting nodes (symbols). Black squares correspond to phage isolated from the phage-amended chemostats, white circles correspond to *Synechococcu*s isolated from phage-amended chemostats, and grey circles correspond to naive *Synechococcus* isolated from no-phage control chemostats. The absence of a line indicates that *Synechococcus* isolates were resistant to phage challenge.

540

542

544

546 **Fig. 3**

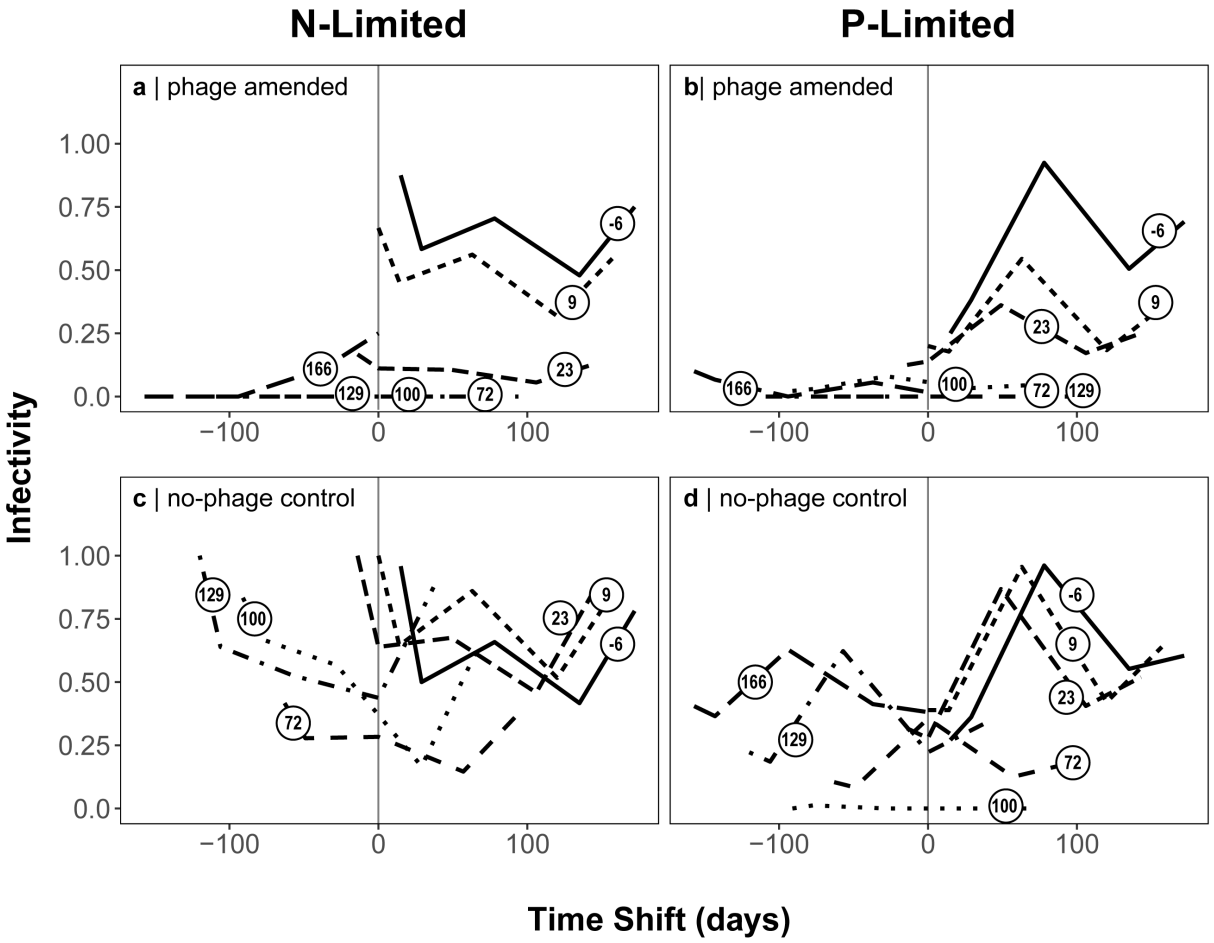

548

Fig. 3. Time-shift analysis of host-phage infectivity reveals the effects of stoichiometry on coevolution. Contemporary interactions (i.e., those between a host and phage strain isolated at the same time point) are centered at time zero (grey vertical line) along the time-shift (horizontal) axis. Interactions with past phage are shifted to the left (negative values) and interactions with future phage are shifted to the right (positive values). Each black line corresponds with the mean infectivity for *Synechococcus* isolated from a specific time point as indicated by the open circle containing the isolation day (-6, 9, 23, 72, 100, 129, or 166). When comparing challenges between hosts and phage from phage-amended chemostats (a, b), infectivity was weak for hosts that were isolated after day 23 or when challenged against phage from the past owing to the evolution of resistance. Such findings are consistent with arms-race dynamics where directional selection gives rise to escalating host resistance. We also challenged phage against naive hosts from the no-phage control chemostats (c, d). From this, we found that infectivity was significantly higher under N-limitation than P-limitation, but overall, was lower than what would be expected under arms race dynamics. Instead, the fluctuations in infectivity with respect to time-shift are consistent with negative frequency-dependent selection and reflect asymmetry in the coevolution between *Synechococcus* and phage.

Fig. 4

550

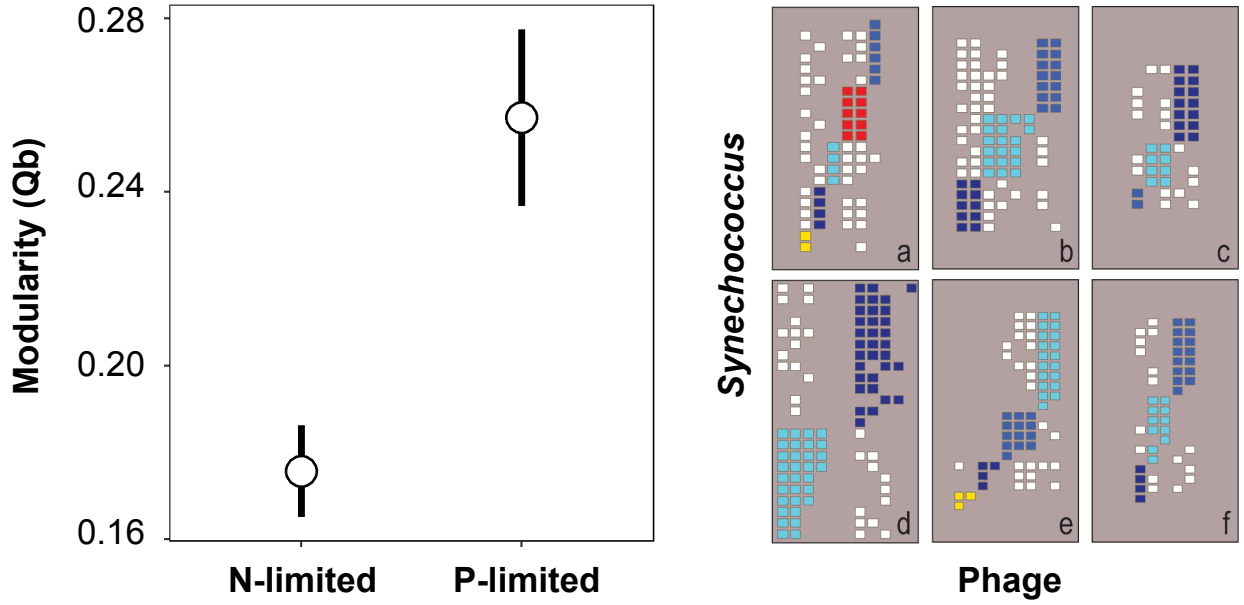

552

Fig. 4. Host-phage infection networks based on interactions between *Synechococcus* and phage isolates that coevolved under N- and P-limitation. Networks were significantly nested, consistent with expectations of host-phage systems coevolving under arms race dynamics. However, the degree of nestedness was not affect by stoichiometry. Left panel: Networks were also significantly modular when compared to randomized networks, but the degree of modularity was significantly greater in P-limited networks. Right panel: Infection networks with interactions (colored cells) rearranged using the LPBrim algorithm in BiWeb to reflect the modular structure. Each colored grouping within a panel corresponds to a calculated module within the interaction network of N-limited (a – c) or P-limited (d – f) chemostats.

554